



Green Synthesis of Ceria Nanoparticles Using Azadirachta Indica Plant Extract: Characterization, Gas Sensing and Antibacterial Studies

**SATISH ARVIND AHIRE¹, ASHWINI ASHOK BACHHAV²,
THANSINGH BHAWSING PAWAR¹, ARUN VITTHAL PATIL³,
SWAPNIL SAMPATRAO SHENDGE⁴ and PRASHANT BHIMRAO KOLI^{5*}**

¹Department of Chemistry, L.V.H. Arts, Science and Commerce College, Panchavati, Nashik, Affiliated to Savitribai Phule Pune University, Pune, Maharashtra, India.

²Maratha Vidyaprasarak Samaj, Institute of Pharmaceutical Science, Nashik. Affiliated to Savitribai Phule Pune University, Pune, Maharashtra, India.

³Department of Physics, Arts, Science and Commerce College, Manmad, District-Nashik, Affiliated to Savitribai Phule Pune University, Pune, Maharashtra, India.

⁴Department of Physics, Karmaveer Abasaheb and N.M. Sonawane Arts Commerce and Science College, Satana, Taluka-Baglan, District- Nashik. Affiliated to Savitribai Phule Pune University, Pune, Maharashtra, India.

⁵Department of chemistry, Karmaveer Abasaheb and N.M. Sonawane Arts Commerce and Science College, Satana, Taluka-Baglan, District- Nashik. Affiliated to Savitribai Phule Pune University, Pune, Maharashtra, India.

Abstract

In the present investigation we have fabricated the cerium dioxide (CeO_2) nanoparticles by green route. While preparing the cerium dioxide nanoparticles by co-precipitation method, Neem leaf extract mixed into the precursor of cerium. The synthesized nanoparticles of CeO_2 were used for the preparation of thick film sensor by using screen printing strategy. The fabricated CeO_2 sensor was characterized by XRD, SEM, EDS and TEM techniques. The structural characteristics investigated by x-ray diffraction technique (XRD). XRD confirms the formation of cubic lattice of CeO_2 material. The surface, texture, porosity characteristics were investigated from SEM analysis, while chemical composition of the material was analysed by EDS technique. The transmission electron microscopy (TEM) confirms the formation cubic lattice of the cerium dioxide material. The thickness of the films was calculated from



Article History

Received: 13 December 2021

Accepted: 30 December 2021

Keywords

Antibacterial Study;
 CeO_2 Sensor; Lpg;
Petrol Vapors Sensor;
Tem.

CONTACT Prashant Bhimrao Koli ✉ prashantkoli005@gmail.com 📍 Department of chemistry, Karmaveer Abasaheb and N.M. Sonawane Arts Commerce and Science College, Satana, Taluka-Baglan, District- Nashik. Affiliated to Savitribai Phule Pune University, Pune, Maharashtra, India.



© 2021 The Author(s). Published by Enviro Research Publishers.

This is an Open Access article licensed under a Creative Commons license: Attribution 4.0 International (CC-BY).

Doi: <http://dx.doi.org/10.13005/msri/180304>

mass difference method, the prepared film sensors belong to thick region. The fabricated material CeO₂ sensor was applied as gas sensor to sense the gases such as LPG, petrol vapors (PV), toluene vapors (TV) and CO₂. The CeO₂ sensor showed excellent gas response for LPG and PV, nearly 93.20 % and 78.23 % gas response. The rapid response and recovery of the prepared sensors was observed at the tested gases. CeO₂ material also employed for antibacterial study at several pathogenic organism such as pseudomonas, staphylococcus aureus and salmonella typhae. From antibacterial study it was observed that the material is capable of inhibiting the growth of these pathogenic microbes.

Introduction

Material science is highly versatile branch which covers almost every field of science and technology. The new materials under the heading of nanotechnology are being reported by the researchers such as nanocomposites, modified semiconductors, transition metal doped materials, nanomaterial synthesis using plant extract etc. There is variety of materials reported by the researchers based on the green chemistry approach. The materials involve fabrication of nanomaterials from leaves, bark, and stem extract etc. Particularly the fabrication of silver and gold nanomaterials by using Azadirachta Indica leaf extract, Madhuca Longifolia extract etc. Some of the researchers reported the fabrication of nanomaterials by using medicinal plant extract, Impatiens balsamina, Lantana camara plant extract etc. to modify some surface characteristics of the nanomaterial. According to the researchers the plant extract fabrication of nanomaterials is able to modify many inherent properties of nanomaterials such as reduction of nanomaterials, enhanced surface rigidity, chemical and physical changes of nanomaterials etc.

Due to the unique physical and chemical properties, the rare earth elements have attracted the attention of the researchers. The term rare related to their difficult process of extraction. The rare earths, cerium is the most abundant metal found in the Earth's crust¹ (about 0.0046 wt%). In the periodic table, Cerium is the first element of the lanthanide series. In 1803, the existence of Ce in an oxide was first reported in Sweden and Germany.² This cerium oxide named as Ceria and it was given by Jacob Berzelius in Sweden. He named this oxide after the dwarf planet ceres, which itself means the Roman Goddess of Agriculture.¹

Uncommon chemical state of cerium dioxide is +4 recognised as ceria. It is a pale yellow/white powder that is formed by the calcination of the cerium oxalate or hydroxide. The 4f orbital of rare earths are shielded by the 5p and 4d electrons, that results in the fascinating catalytic properties.³⁻⁵ Cerium exist in both +III and +IV oxidation states.¹ Thus, in bulk state it exists as CeO₂ and Ce₂O₃. CeO₂ nanomaterial contains a mix of cerium in the +III and +IV chemical states on the surface of the nanoparticle.⁶ As the diameter of the nanoparticle decreases, the number of +III sites on the surface increases, that results in the loss of oxygen atoms (Oxygen vacancies).⁷⁻⁸ CeO₂ has gained much attention in the field of nanotechnology due to their useful application for catalysts, fuel cells and fuel additives. Nanoceria (Cerium oxide nanoparticles) are widely used in chemical mechanical polishing,⁹ solar cells,¹⁰ fuel oxidation catalysis,¹¹ as catalyst or non-inert support catalyst and in the construction of the three way catalysts, and automotive exhaust treatment.¹² Due to lower toxicity, they also have been used as antitumor,¹³ antioxidant,¹⁴ anti-inflammation,¹⁵ antibacterial.¹⁶ in combating neurodegenerative diseases and as immunosensors.¹⁷ Recently, there are many reviews are published on the cerium and cerium oxides focusing on the synthesis,¹⁸ defect engineering,¹⁹ catalysis,²⁰ pharmaceutical properties,²¹ biological and biomedical effects.²²

There are many toxic and fatal effects have been reported so far due to gas leakage and more concentration of toxic gas vapors like carbon monoxide, nitrogen dioxide, carbon dioxide etc. The reagent such as toluene is toxic to its threshold limit and hence the concentration of these gas vapors must be regulated through efficient gas

sensors. The metal oxide based gas sensors are more efficient, easy to fabricate, low cost and easy to operate hence most of the researchers are diverted their attention to develop good, stable and reproducible sensors that can be operated at low temperature and are able to sense the toxic gases at lower concentration.²³⁻²⁶

The present study deals with synthesis of CeO₂ nanoparticles by using Azadirachta Indica (Neem) leaf extract. The method belongs to the green synthesis method, which is low cost, facile and non-toxic method to fabricate the ceria nanoparticles. The fabricated green ceria nanoparticles were characterized by essential nano characterization techniques. Further, the prepared ceria nanoparticles were utilized as gas sensor material for some toxic gases such as (CO₂), (NO₂), C₆H₅-CH₃, and petrol vapors (PV) etc. Additionally the material was utilized for antibacterial application of several pathogenic organisms.

Materials and Methods

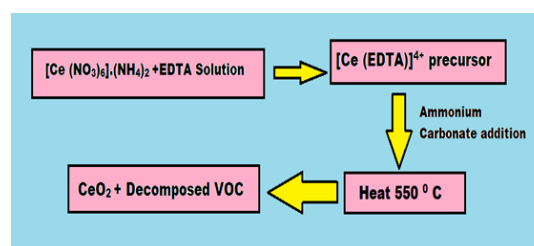
Precursors used in the green fabrication of CeO₂ nanoparticles were of analytical grade reagents and utilized without further purification. The chemicals used were, Ceric ammonium nitrate (CAN), ethylene diamine tetra acetic acid (EDTA), ammonium carbonate. Azadirachta Indica Neem (AIN) dried leaves were taken from local trees of nearby region of Nashik.

Fabrication of CeO₂ (Cerium Dioxide) Nanoparticles by using Azadirachta Indica Neem (Ain) leaf extract

For fabrication of cerium dioxide nanoparticles initially the solution of Ceric ammonium nitrate (CAN) was prepared with 0.01 M in 70 cm³ water. EDTA solution with 0.02 M was prepared in 50 ml of water. The 0.01 M CAN solution was kept over the magnetic stirrer, the magnetic niddle was kept in the solution. The magnetic stirrer was set at 1000 rpm and 50°C temperature to initiate the reaction with faster rate. To this 0.01M CAN solution the previously prepared AIN leaf extract (10 ml) solution mixed. To, this above mixture solution, slowly 0.02 M EDTA solution was added. After complete addition of EDTA, the 0.1 M NH₄CO₃ solution was mixed. The NH₄CO₃ solution was added to control the size of nanoparticles formed and prevents the reverse reaction. This overall mixture was continuously

stirred for two hours. Then, the pale yellow precipitate was obtained; filter through whatmann filter paper 41. The obtained precipitates were then dried in hot air oven at 70°C for 30 minutes. The obtained precipitates were fired in muffle furnace at 550°C for 180 minutes; the faint yellow coloured CeO₂ nanoparticles were obtained.²⁷⁻³²

The formation of CeO₂ chemical reaction is as depicted in scheme-1



Scheme-1 Synthesis of Cerium oxide nanoparticles

Azadirachta Indica Neem (AIN) leaf extracts development

The AIN leaf extract was prepared by mixing 15g of Neem leaves in electric mixer machine. The grinded Neem leaves extract was then mixed up in one litre beaker containing distilled water. The water containing Neem leaves extract was allowed to boil at 70°C for 30 minutes. Then, the Neem leaf extract was centrifuged in a centrifuge machine at 2000 rpm for 20 minutes so that the sediment Neem leaf extract and supernant liquid should be separated. Finally, the Neem leaf extract was filtered out. The extract was kept in refrigerator for further use.

Preparation of thick films of CeO₂ (Cerium dioxide)

The film sensor of CeO₂ material was fabricated by Neem leaf extract using standard screen printing strategy. In this method the fabricated CeO₂ nanoparticles were used to prepared thick films. The material such as ethyl cellulose (EC), butyl carbitol acetate (BCA) used to design the film sensors considered as an organic part employed as binders. This inorganic to organic molecule ratio was kept as 70:30 respectively. Inorganic material CeO₂ was added in mechanical mixer (700 mg) and grinded half hour. Then pinch of EC was added in mortar pestle containing CeO₂ nanoparticles.

Then BCA was added drop wise to the grinded CeO₂ nanoparticles. The whole composite was stirred in Mortar pestle till the thixotropic phase (gel type) was achieved. This paste was pasted over the glass substrate, by means of photolithography technique. The screen surface made from organic polymer nylon with 42 s, size 356 was utilized for designing CeO₂ film sensor.³³⁻³⁶ After, complete coating of the films, the films were dried at room temperature and then films were fired in muffle furnace at 400°C.

Thickness measurement of CeO₂ film sensor

The film sensor thickness was calculated by weight difference method, using equation 1. By solving equation 1 as per obtained data, the thickness of the CeO₂ was 4.312 μm (4312 nm).

The thickness of the film sensor was obtained in the thick region.

$$t = \Delta W / A \times \rho \quad \dots(1)$$

Where $\Delta W = W_2 - W_1$

W_1 = Mass of sensor before deposition, W_2 = Mass of the sensor after deposition.

A = (Breadth * Height = 2 cm * 1.5 cm = 3.0 cm²),
 ρ = Composite density of CeO₂ material.

Results and Discussions

X-ray Diffraction study

The fabricated material CeO₂ material was characterized by XRD method. The XRD technique was utilized to get structural characteristics of the CeO₂ material. The XRD pattern of CeO₂ material is as represented in Figure 1. MoK α material was utilized to generate X-rays, having intensity of 1.54 Å⁰. The Braggs diffraction peaks can be refer to the formation of cerium oxide nanoparticles such as 28.93°, 33.45°, 47.83°, 56.66°, 59.40°, 69.67°, 76.91°, 79.47° that are assign to the Braggs planes represented in figure 1. From XRD analysis, the formation of CeO₂ nanoparticles was confirmed. The average nanoparticle size of CeO₂ material was computed from equation 2.

$$D = K\lambda / \beta \cos \theta \quad \dots(2)$$

The mean nanoparticle size of cerium nanoparticles calculated using equation 2 was 30.57 nm.

The XRD pattern of the fabricated material CeO₂ shows matching data with 750390 JCPDS card number.

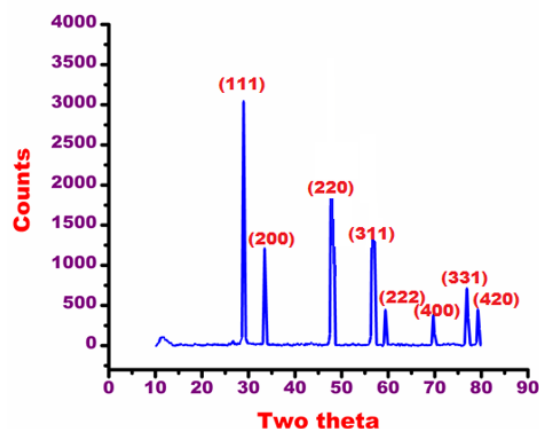


Fig.1: XRD spectrum of fabricated CeO₂

Scanning Electron microscopy (SEM)

The surface characteristics of CeO₂ material fabricated by Azadirachta Indica (Neem) leaf extract is shown in Figure 2 a-d. The images shows the surface characteristics such as texture, porosity and material topography can be seen from these images. From SEM images a-d it can be visualise that the material CeO₂ has homogeneous surface. The different dimensions grains with varied size are visible from SEM images. From image b and d it can be seen that the surface consists of small voids or cavities or interstitial spaces that exhibits that the material is porous in nature. The small cavities present over the surface of this material have many merits from chemical reactivity point of view. Since the voids are very useful for adsorption phenomenon.³⁷⁻³⁹ The design sensor CeO₂ was utilized as gas sensor, thus, these cavities plays vital role to accommodate smaller gas moieties such that there may be maximum interaction between adsorbate gas molecules and adsorbent sensor. Additionally, the material also demonstrates that there is close agglomeration of smaller grains together which are useful for adsorption characteristics.

Energy dispersive spectroscopy (EDS) study

EDS spectrum of fabricated material CeO₂ is as depicted in Figure 3. EDS analysis of the material was carried out to get the elemental composition of material. The composition of the fabricated

CeO₂ material is as depicted in embedded table in figure 3. Figure 3 represents the characteristic peak of elemental cerium observed at 5.0 KeV. The EDS

results confirm the successful fabrication of ceria nanoparticles.⁴⁰

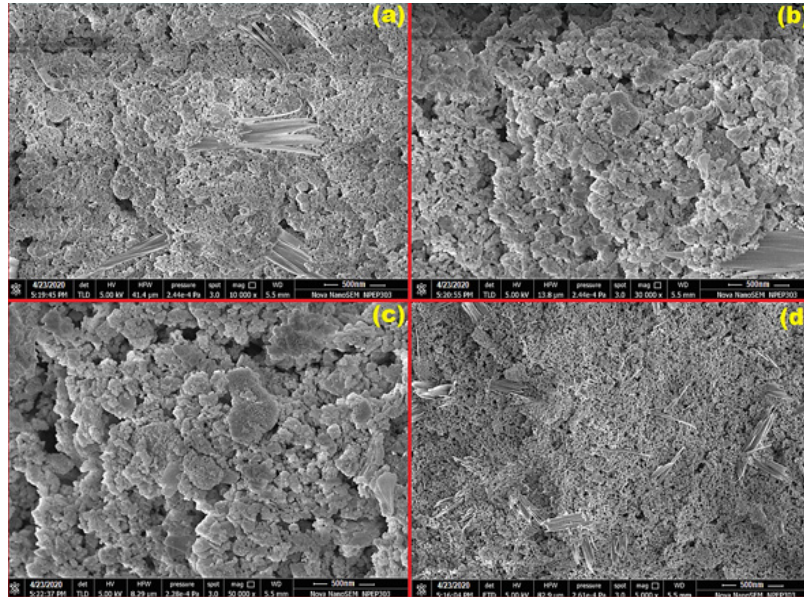


Fig. 2 : SEM images of fabricated CeO₂ material calcined at 400°C

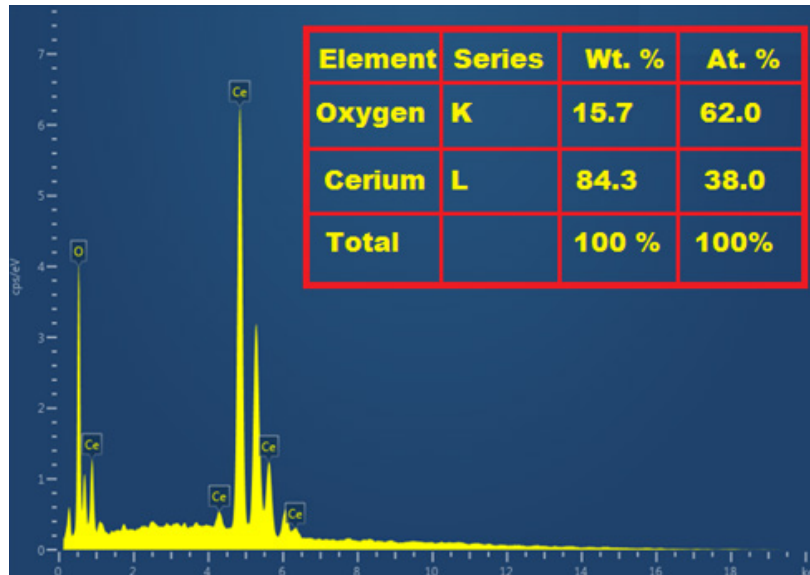


Fig. 3 : EDS spectrum of fabricated CeO₂ material

High resolution transmission electron microscopy (HR-TEM)

The material CeO₂ was analysed by HR-TEM technique for crystal lattice information and type of substance synthesized. The HR-TEM of the CeO₂ material is as depicted in Figure 4. The cerium

oxide belongs to cubic arrangement; the figure a-d shows the TEM images of the cerium oxide material. The images demonstrate roughly cubic lattice for the fabricated CeO₂ material. The figure 4-a shows inter-planar distance of 0.28 nm of the grain particles. Figure 4-b shows the different size of grain crystals

of CeO₂ material. The SAED pattern for the material is reported in the figure 4-d, represents diffraction pattern for the material. The dark spots appear

in the ring form shows that material belongs to polycrystalline nature.⁴¹⁻⁴⁴

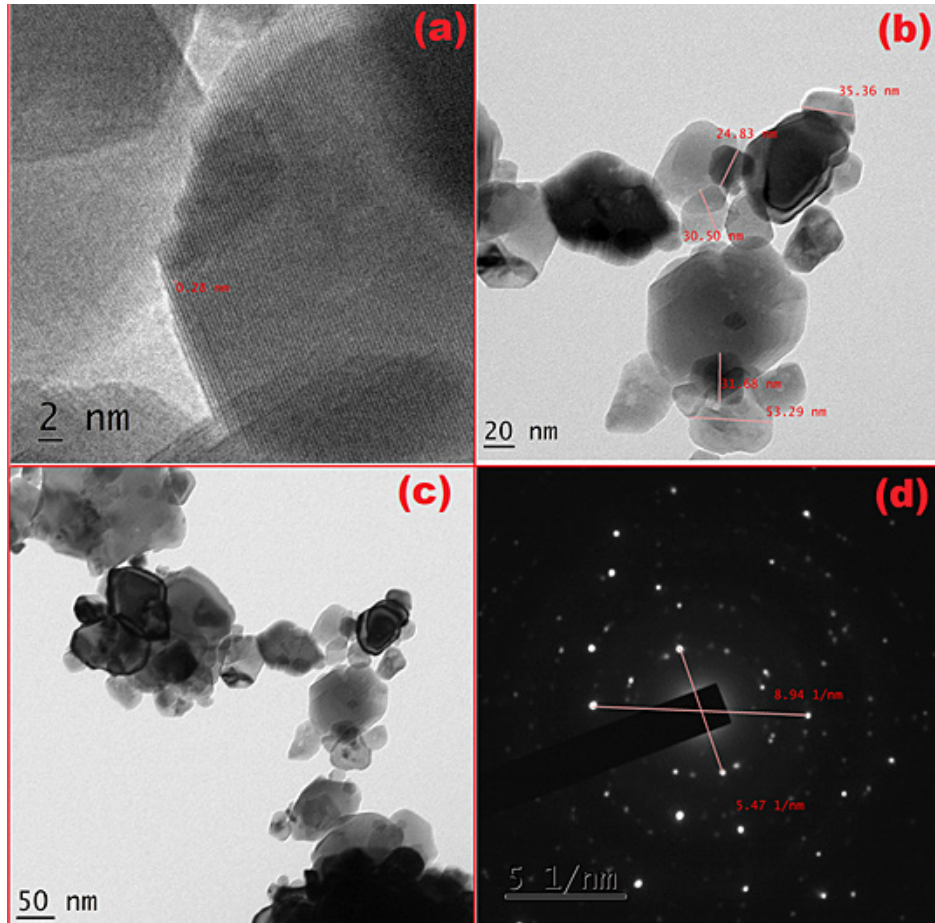


Fig. 4 : (a-c) HR-TEM images of fabricated CeO₂ material, (d) selected area electron diffraction (SAED) pattern of CeO₂ material

Gas sensing study of cerium oxide (CeO₂) sensor

The fabricated thick film sensor CeO₂ was utilized as a sensor material for some toxic gases, such as toluene vapors (C₆H₅-CH₃), CO₂, LPG and petrol vapors. The sensing mechanism was performed with the aid of gas sensing unit represented in Figure 5. For obtaining typical gas response (S) using CeO₂ sensor, the electrical resistance of the film sensor was recorded in the air atmosphere (Ra) and in gaseous environment (Rg). The gas response was evaluated from equation 3 as given below-----

$$S\% = \frac{R_a - R_g}{R_a} \times 100 \quad \dots(3)$$

R_a= Resistance in oxygen atmosphere,
R_g= Resistance in gas atmosphere

The gas response (sensitivity) of the tested gases is as depicted in Figure 6-a. The gas sensitivity was recorded for the toluene vapors (C₆H₅-CH₃), CO₂, LPG and petrol vapors. All the above listed gases have fatal effects over environment. Hence their concentration must be regulated by developing some acute sensors. Here the resistance of the film sensor was calculated by recording change in voltage against the constant resistance. The voltage across fixed resistance is mutually

convertible and measure by means of Ohm's law ($V=IR$). The change in resistance with elevated temperature was recorded by digital multimeter. For each cycle calculated amount of testing vapors (ppm) was allowed to enter into glass chamber, change voltage due to interaction between gas vapors and surface of metal oxide film was recorded with multimeter. After successful gas sensing cycle, the gas concentration was removed through the temperature supplement from thermostat.⁴⁵⁻⁴⁷

CeO₂ sensor was successfully employed to sense the gases above listed out of that it showed highest response to the liquefied petroleum gas (LPG) vapors. For LPG vapors 93.25 % gas response at 150°C was recorded. Simultaneously, the sensor showed 78.20 % gas response for petrol vapors (PV) at 200°C, then 70.26 % gas response for toluene vapors (TV) at 200 °C and 52.48% gas response at 250°C gas response was recorded. The good gas sensing results of CeO₂ is attributed to the porous nature, moderate band gap and good surface area of the cerium dioxide sensor. The gas response with change in temperature is as depicted in Figure 6-b.

The sensor initially tested for the gases with the different gas concentration from 10¹ to 10³ gas ppm concentration. The variation of sensitivity against the vapors concentration is given in Figure 6-a. For increasing gas concentration the response signal is found to be enhanced. But further increasing the gas concentration beyond 600 ppm the gas response signal is found to be declined, the observation suggest the saturation tendency of the sensor towards tested gases at higher

concentration of the tested gases. Percent selectivity of fabricated sensor cerium dioxide computed from equation 4.

$$\% \text{ Selectivity} = (S_{\text{other gas}} / S_{\text{target gas}}) * 100 \quad \dots(4)$$

S_{target gas} – Gas response for high responded gas

S_{other gas} - Gas response for other tested gases

For effective working of the sensor, it must obey the conditions such as stability, rapid response and recovery, fast sensitivity, good accessibility for the testing gases, and its reusability performance. The fabricated sensor cerium dioxide was tested for the reusability test in four cycles with time of 40 days in four runs. The test was performed at 600 ppm gas concentration for LPG and petrol vapors (PV). The results obtained from reusability test for total 4 cycles with the overall time period 40 days shown in Table 1. From table 1 it can be observed that fabricated sensor is effective to produce the gas response with frequent utilization of the sensor with specific time interval. Here, in general observation it was observed that for every run (with time interval of days) the gas response was found to declined very slightly. The declined in the gas response at every run is due to the dwindle in surface active properties of the sensor due to frequent interaction between gas vapors and sensor material. Although the reproducibility results are very satisfactory for the tested gases LPG and petrol vapors (PV), hence the fabricated sensor is reliable to sense these gases.⁴⁸⁻⁵⁰

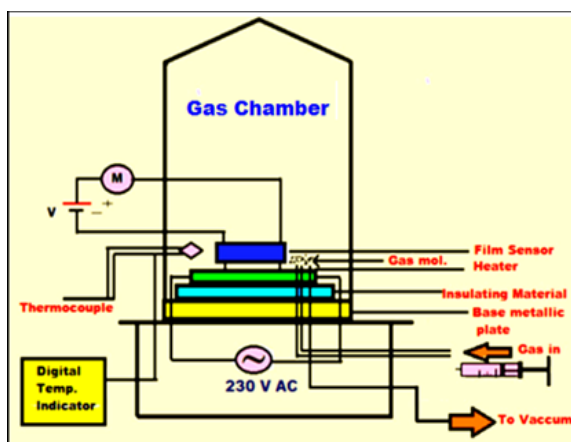


Fig. 5 : Block diagram for gas sensing study

Table 1: Reproducibility results for LPG and PV at CeO₂ sensor

Time Interval (In days)	Number of cycle	Gas response % (LPG)	Gas response % (PV)
10	I	93.20	78.23
20	II	91.22	76.32
30	III	89.30	74.42
40	IV	87.26	72.56

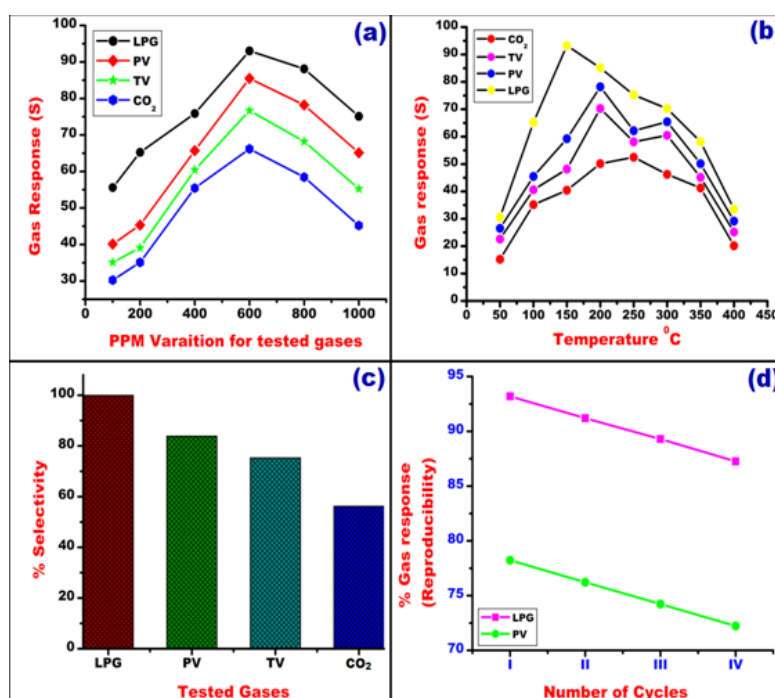


Fig. 6 : (a) PPM variation of tested gases at CeO₂ sensor, (b) Gas response of tested gases at CeO₂ sensor, (c) % Selectivity of tested gases towards CeO₂ sensor, (d) reproducibility results for LPG and Petrol vapors at CeO₂ sensor

Table 2: Response and recovery study for CeO₂ sensor at LPG and PV gases

Design material	Investigated gas	Gas response	Response Time (sec.)	Recovery Time (sec.)
CeO ₂ sensor	LPG	93.20	21	45
CeO ₂ sensor	PV	78.20	22	42

Response and recovery of CeO₂ sensor for LPG and PV gases

The reliability of the tested results is can be conform from by the response and recovery given by the sensor. This is prime tool to decide the effective working of the sensor in multiple runs. This test is associated with the smooth working of the sensor

at desire temperature and concentration of the tested gases. The fabricated material CeO₂ sensor was effectively utilized for this parameter at the gases LPG and PV. In this research this parameter was tested for LPG and PV gas vapors. Both these tested gases have very rapid recovery and gas sensitivity time at the fabricated CeO₂ sensor.

The response and recovery time for the tested sensor is as depicted in Table 2. The response and recovery curves for LPG and petrol vapors are as shown in Figure 7.

The zone of inhibition around each well indicated that the material effectively worked as antibacterial agent for tested pathogenic microbes.

Antibacterial study by agar well diffusion method

The antibacterial study over the prepared material CeO_2 was performed by means of agar well diffusion method. The pathogenic microorganism suspension was gained from local microbiological laboratory. The organism such as *pseudomonas*, *staphylococcus aureus* and *salmonella typhae* were used in antibacterial study. The antibacterial study was performed using standard agar well diffusion method. Initially the petriplates were marked as catalyst (CeO_2 material) loading from 100 $\mu g/ml$, 200 100 $\mu g/ml$, 300 100 $\mu g/ml$, and 400 100 $\mu g/ml$ for 4 different petriplates. Agar media was uniformly speared over the plates in the form nutrient broth. The agar-agar media was spread uniformly into plates with the aid of L-shaped glass mixer. Then into different quadrants the different organism suspension spread uniformly. The 6 mm cork borer was utilized prepare the wells over the bacterial broth suspension. Three different bacterial suspension were dropped into different well (quadrant) from 100 $\mu g/ml$ to 400 $\mu g/ml$ CeO_2 - Azadirachta Indica (Neem) extract into 4 different plates. After that these all 4 plates were incubated at 38°C for one day. After this incubation period, the clear zone of inhibition (ZOI) was observed around the entire well in petri plates. The ZOI was found maximum in 400 $\mu g/ml$ CeO_2 - Azadirachta Indica concentrations.

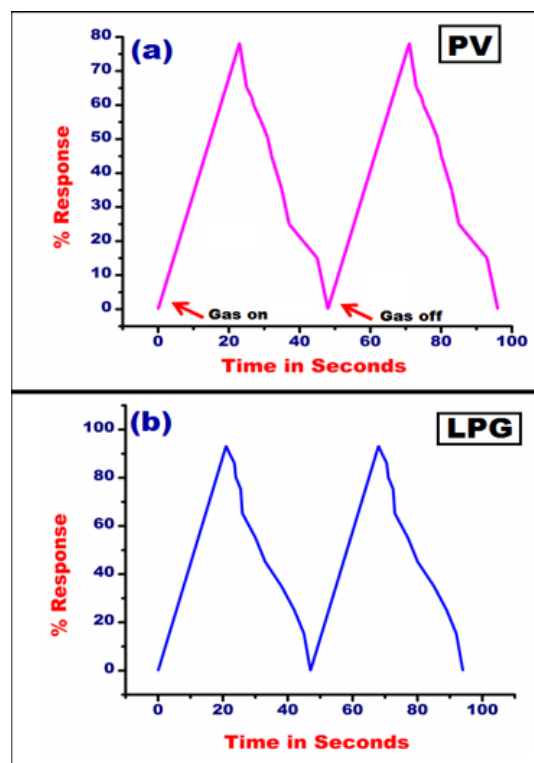


Fig. 7 : (a) Response and recovery curves for PV gas vapors for CeO_2 sensor, (b) Response and recovery curves for LPG gas vapors for CeO_2 sensor

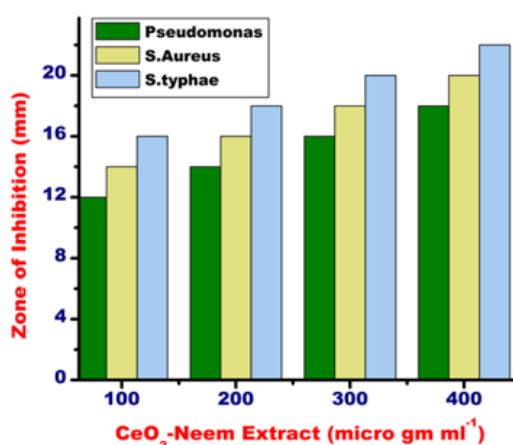


Fig. 8 : antibacterial activity of CeO_2 material fabricated using Azadirachta Indica (Neem) extract against some pathogenic microbes using agar well diffusion method

Conclusions

The CeO₂ material was exclusively utilized as a gas sensor for LPG, petrol vapors (PV), toluene vapors (TV) and CO₂. From above tested gases the fabricated sensor showed good response for LPG and petrol vapors at 600 ppm gas concentration. The LPG vapors showed 93.20% and PV showed 78.20 % gas response at moderately high temperature. From the response recovery and reproducibility results the material CeO₂ sensor is very promising, effective and stable sensor to sense the hazardous gases such as LPG and petrol vapors at considerably low concentrations. Additionally, the CeO₂ material was investigated for antibacterial study. The material was found to inhibit growth of the pathogenic microbes. From the obtained results it can be concluded that the fabricated material CeO₂ multifaceted material which is can be used in the environmental applications as well as microbiological applications.

Acknowledgments

Authors are gratefully acknowledged to the STIC, Cochin University, Kerala for XRD, TEM results. Authors are also gratefully acknowledged to STIC, Cochin University, Kerala SEM and EDS results. Authors are grateful to Department of Chemistry, L.V.H. College, Panchavati, Nashik (MAH, India) for providing necessary laboratory facilities. Authors are also grateful to Department of Chemistry, K.A.A.N.M.S, Department of Chemistry, ACS, College, Satana, District- Nashik, (MAH, India), for providing necessary laboratory facilities.

Funding

Authors have not received any funding or grant from any institute for the present research

Conflict of Interest

Authors declare that they have no conflict of interest for the present research.

References

1. Dahle JT, Arai Y. Environmental geochemistry of cerium: Applications and toxicology of cerium oxide nanoparticles. *Int J Environ Res Public Health*. 2015;12(2):1253-1278. doi:10.3390/ijerph120201253
2. Weeks ME. The discovery of the elements. XVI. the rare earth elements. *J Chem Educ*. 1932;9(10):1751-1773. doi:10.1021/ed009p1751
3. Patil MP, Singh RD, Koli PB, Patil KT, Jagdale BS, Tipare AR, Kim GD. Antibacterial potential of silver nanoparticles synthesized using Madhuca longifolia flower extract as a green resource. *Microbial pathogenesis*. 2018, 1;121:184-9.
4. Shinde VS, Kapadnis KH, Sawant CP, Koli P.B, Patil RP. Screen Print Fabricated In 3+ Decorated Perovskite Lanthanum Chromium Oxide (LaCrO₃) Thick Film Sensors for Selective Detection of Volatile Petrol Vapors. *Journal of Inorganic and Organometallic Polymers and Materials*. 2020, 30(12):5118-32.
5. Koli PB, Kapadnis KH, Deshpande UG, pandurang More B, Tupe UJ. Sol-Gel Fabricated Transition Metal Cr³⁺, Co²⁺ Doped Lanthanum Ferric Oxide (LFO-LaFeO₃) Thin Film Sensors for the Detection of Toxic, Flammable Gases: A Comparative Study. *Material Science Research India*. 2020, 30;17(1):70-83.
6. Koli PB, Kapadnis KH, Deshpande UG, Tupe UJ, Shinde SG, Ingale RS. Fabrication of thin film sensors by spin coating using sol-gel LaCrO₃ Perovskite material modified with transition metals for sensing environmental pollutants, greenhouse gases and relative humidity. *Environmental Challenges*. 2021 Apr 1;3:100043.
7. Song S, Wang K, Yan L, et al. Ceria promoted Pd/C catalysts for glucose electrooxidation in alkaline media. *Appl Catal B Environ*. 2015;176-177:233-239. doi:10.1016/j.apcatb.2015.03.059
8. Montini T, Melchionna M, Monai M, Fornasiero P. Fundamentals and Catalytic Applications of CeO₂-Based Materials. *Chem Rev*. 2016;116(10):5987-6041. doi:10.1021/acs.chemrev.5b00603
9. Cedric Bouzigues, Thierry Gacoin and AA. Biological Applications of Rare-Earth Based Nanoparticles. *NMR EPR Spectrosc*. 2011;(11):8488-8505. doi:10.1016/b978-1-4832-1326-2.50022-9

10. Tereshchuk P, Freire RLH, Ungureanu CG, Seminovski Y, Kiejna A, Da Silva JLF. The role of charge transfer in the oxidation state change of Ce atoms in the TM13-CeO₂ (111) systems (TM = Pd, Ag, Pt, Au): A DFT + U investigation. *Phys Chem Chem Phys*. 2015;17(20):13520-13530. doi:10.1039/c4cp06016d
11. Koli PB, Kapadnis KH, Deshpande UG. Study of physico-chemical properties, detection and toxicity study of organic compounds from effluent of MIDC Thane and GIDC Ankleshwar industrial zone. *Applied Water Science*. 2018 Nov;8(7):1-9.
12. Bagul VR, Bhagure GR, Ahire SA, Patil AV, Adole VA, Koli PB. Fabrication, characterization and exploration of cobalt (II) ion doped, modified zinc oxide thick film sensor for gas sensing characteristics of some pernicious gases. *Journal of the Indian Chemical Society*. 2021 Nov 1;98(11):100187.
13. Waghchaure RH, Koli PB, Adole VA, Pawar TB, Jagdale BS. Transition metals Fe³⁺, Ni²⁺ modified titanium dioxide (TiO₂) film sensors fabricated by CPT method to sense some toxic environmental pollutant gases. *Journal of the Indian Chemical Society*. 2021 Sep 1;98(9):100126.
14. Ahire SA, Koli PB, Patil AV, Jagdale BS, Bachhav AA, Pawar TB. Designing of screen-printed stannous oxide (SnO₂) thick film sensors modified by cobalt and nitrogen elements for sensing some toxic gases and volatile organic compounds. *Current Research in Green and Sustainable Chemistry*. 2021 Nov 9:100213.
15. Koli PB, Shinde SG, Kapadnis KH, Patil AP, Shinde MP, Khairnar SD, Sonawane DB, Ingale RS. Transition metal incorporated, modified bismuth oxide (Bi₂O₃) nano photo catalyst for deterioration of rosaniline hydrochloride dye as resource for environmental rehabilitation. *Journal of the Indian Chemical Society*. 2021 Oct 28:100225.
16. Tsunekawa S, Sivamohan R, Ito S, Kasuya A, Fukuda T. Structural study on monosize CeO₂-X nano-particles. *Nanostructured Mater*. 1999;11(1):141-147. doi:10.1016/S0965-9773(99)00027-6
17. Tsunekawa S, Sivamohan R, Ohsuna T, Kasuya A, Takahashi H, Tohji K. Ultraviolet absorption spectra of CeO₂ nano-particles. *Mater Sci Forum*. 1999;315-317:439-445. doi:10.4028/www.scientific.net/MSF.315-317.439
18. Reed K, Cormack A, Kulkarni A, et al. Exploring the properties and applications of nanoceria: Is there still plenty of room at the bottom? *Environ Sci Nano*. 2014;1(5):390-405. doi:10.1039/c4en00079j
19. Corma A, Atienzar P, García H, Chane-Ching JY. Hierarchically mesostructured doped CeO₂ with potential for solar-cell use. *Nat Mater*. 2004;3(6):394-397. doi:10.1038/nmat1129
20. Jung H, Kittelson DB, Zachariah MR. The influence of a cerium additive on ultrafine diesel particle emissions and kinetics of oxidation. *Combust Flame*. 2005;142(3):276-288. doi:10.1016/j.combustflame.2004.11.015
21. Campbell CT, Peden CHF. Oxygen vacancies and catalysis on ceria surfaces. *Science* (80-). 2005;309(5735):713-714. doi:10.1126/science.1113955
22. Corsi F, Caputo F, Traversa E, Ghibelli L. Not only redox: The multifaceted activity of cerium oxide nanoparticles in cancer prevention and therapy. *Front Oncol*. 2018;8(AUG):1-7. doi:10.3389/fonc.2018.00309
23. Kim SJ, Chung BH. Antioxidant activity of levan coated cerium oxide nanoparticles. *Carbohydr Polym*. 2016;150:400-407. doi:10.1016/j.carbpol.2016.05.021
24. Patil A.P, Ahire SA, Hiray SN, Kapadnis KH, Rajput TA, Koli P.B. Enhanced Photocatalytic Activity of two Dimensional Graphitic C₃N₄@ Co₃O₄ Core Shell Nanocomposite for Discriminatory Organic Transformation of CF dye under Hg-vapor Reactor. *Material Science Research India*. 2021 Aug 31;18(2):190-205.
25. Shinde RS, More RA, Adole VA, Koli PB, Pawar TB, Jagdale BS, Desale BS, Sarnikar YP. Design, fabrication, antitubercular, antibacterial, antifungal and antioxidant study of silver doped ZnO and CuO nano candidates: A comparative pharmacological study. *Current Research in Green and Sustainable Chemistry*. 2021 Jan 1;4:100138.
26. Waghchaure RH, Koli PB, Adole VA, Jagdale BS, . Transition Metals Ni²⁺, Fe³⁺ Incorporated Modified ZnO Thick Film Sensors to Monitor the Environmental and

- Industrial Pollutant Gases. *Oriental Journal of Chemistry*. 2020;36(6):1049-65.
27. Koli PB, Kapadnis KH, Deshpande UG. Nanocrystalline-modified nickel ferrite films: an effective sensor for industrial and environmental gas pollutant detection. *Journal of Nanostructure in Chemistry*. 2019 Jun;9(2):95-110.
28. Huang X, Li LD, Lyu GM, et al. Chitosan-coated cerium oxide nanocubes accelerate cutaneous wound healing by curtailing persistent inflammation. *Inorg Chem Front*. 2018;5(2):386-393. doi:10.1039/c7qi00707h
29. Arumugam A, Karthikeyan C, Haja Hameed AS, Gopinath K, Gowri S, Karthika V. Synthesis of cerium oxide nanoparticles using *Gloriosa superba* L. leaf extract and their structural, optical and antibacterial properties. *Mater Sci Eng C*. 2015;49:408-415. doi:10.1016/j.msec.2015.01.042
30. Naz S, Beach J, Heckert B, et al. Cerium oxide nanoparticles: A "radical" approach to neurodegenerative disease treatment. *Nanomedicine*. 2017;12(5):545-553. doi:10.2217/nnm-2016-0399
31. Nyoka M, Choonara YE, Kumar P, Kondiah PPD, Pillay V. Synthesis of cerium oxide nanoparticles using various methods: Implications for biomedical applications. *Nanomaterials*. 2020;10(2). doi:10.3390/nano10020242
32. Seal S, Jeyaranjan A, Neal CJ, Kumar U, Sakthivel TS, Sayle DC. Engineered defects in cerium oxides: Tuning chemical reactivity for biomedical, environmental, & energy applications. *Nanoscale*. 2020;12(13):6879-6899. doi:10.1039/d0nr01203c
33. Walkey C, Das S, Seal S, et al. Catalytic properties and biomedical applications of cerium oxide nanoparticles. *Environ Sci Nano*. 2015;2(1):33-53. doi:10.1039/c4en00138a
34. Xu C, Qu X. Cerium oxide nanoparticle: A remarkably versatile rare earth nanomaterial for biological applications. *NPG Asia Mater*. 2014;6(3):e90-16. doi:10.1038/am.2013.88
35. Dhall A, Self W. Cerium oxide nanoparticles: A brief review of their synthesis methods and biomedical applications. *Antioxidants*. 2018;7(8):1-13. doi:10.3390/antiox7080097
36. Zhang M, Zhang C, Zhai X, Luo F, Du Y, Yan C. Antibacterial mechanism and activity of cerium oxide nanoparticles. *Science China Materials*. 2019, 62(11):1727-39.
37. Babu KS, Anandkumar M, Tsai TY, Kao TH, Inbaraj BS, Chen BH. Cytotoxicity and antibacterial activity of gold-supported cerium oxide nanoparticles. *International journal of nanomedicine*. 2014;9:5515.
38. Arumugam A, Karthikeyan C, Hameed AS, Gopinath K, Gowri S, Karthika V. Synthesis of cerium oxide nanoparticles using *Gloriosa superba* L. leaf extract and their structural, optical and antibacterial properties. *Materials Science and Engineering: C*. 2015 Apr 1;49:408-15.
39. Khadar YS, Balamurugan A, Devarajan VP, Subramanian R. Hydrothermal synthesis of gadolinium (Gd) doped cerium oxide (CeO₂) nanoparticles: characterization and antibacterial activity. *Oriental Journal of Chemistry*. 2017;33(5):2405.
40. Roudbaneh SZ, Kahbasi S, Sohrabi MJ, Hasan A, Salihi A, Mirzaie A, Niyazmand A, Nanakali NM, Shekha MS, Aziz FM, Vaghar-Lahijani G. Albumin binding, antioxidant and antibacterial effects of cerium oxide nanoparticles. *Journal of Molecular Liquids*. 2019, 15;296:111839.
41. Balamurugan A, Sudha M, Surendhiran S, Anandarasu R, Ravikumar S, Khadar YS. Hydrothermal synthesis of samarium (Sm) doped cerium oxide (CeO₂) nanoparticles: characterization and antibacterial activity. *Materials Today: Proceedings*. 2020 Jan 1;26:3588-94.
42. Rajeshkumar S, Naik P. Synthesis and biomedical applications of cerium oxide nanoparticles—a review. *Biotechnology Reports*. 2018, 1;17:1-5.
43. Zhang H, Qiu J, Yan B, Liu L, Chen D, Liu X. Regulation of Ce (III)/Ce (IV) ratio of cerium oxide for antibacterial application. *Iscience*. 2021, 19;24(3):102226.
44. Kızılkonca E, Torlak E, Erim FB. Preparation and characterization of antibacterial nano cerium oxide/chitosan/hydroxyethylcellulose/polyethylene glycol composite films. *International Journal of Biological Macromolecules*. 2021, 30;177:351-9.
45. Muthuvel A, Jothibas M, Mohana V, Manoharan C. Green synthesis of cerium

- oxide nanoparticles using *Calotropis procera* flower extract and their photocatalytic degradation and antibacterial activity. *Inorganic Chemistry Communications*. 2020 1;119:108086.
46. Senthilkumar RP, Bhuvaneshwari V, Malayaman V, Chitra G, Ranjithkumar R, Dinesh KP, Chandarshekar B. Biogenic method of cerium oxide nanoparticles synthesis using wireweed (*Sida acuta* Burm. f.) and its antibacterial activity against *Escherichia coli*. *Materials Research Express*. 2019, 9;6(10):105026.
47. Agarwal C, Aggrawal S, Dutt D, Mohanty P. Cerium oxide immobilized paper matrices for bactericidal application. *Materials Science and Engineering: B*. 2018, 1;232:1-7.
48. Dai X, Wang X, Chen X, Ye L, Wu M. Fabrication of ultrasound-mediated cerium oxide nanoparticles for the examinations of human osteomyelitis and antibacterial activity. *Applied Nanoscience*. 2021, 11(10):2549-60.
49. Vanitha M, Joni IM, Camellia P, Balasubramanian N. Tailoring the properties of cerium doped zinc oxide/reduced graphene oxide composite: Characterization, photoluminescence study, antibacterial activity. *Ceramics International*. 2018, 1;44(16):19725-34.
50. Sargia B, Shah J, Singh R, Arya H, Shah M, Karakoti AS, Singh S. Phosphate-dependent modulation of antibacterial strategy: a redox state-controlled toxicity of cerium oxide nanoparticles. *Bulletin of Materials Science*. 2017;40(6):1231-40.